by Shinji Sassa[1]*, Hajime Naruse[2], David Tappin[3], and Andreas Roulund[4]

Submarine geohazards and mitigation concept for offshore wind

[1] National Institute of Maritime, Port and Aviation Technology, Port and Airport Research Institute, Yokosuka, Japan; *Corresponding Author, *E-mail: sassa@p.mpat.go.jp*
[2] Kyoto University, Kyoto, Japan
[3] British Geological Survey, Keyworth, Nottingham, UK
[4] Ørsted, Gentofte, Denmark

(Received: November 21, 2025; Revised accepted: May 4, 2026; Online published: June 1, 2026)

https://doi.org/10.18814/epiiugs/2026/02602s02

This paper presents and discusses the characteristics, mechanism, prediction and assessment of submarine geohazards with a special emphasis on liquefaction, coastal and submarine landslides, and tsunamis. Submarine landslide tsunamis are now seen from all geological environments including passive, convergent and transform margins, as well as volcanoes. The typhoons/cyclones/hurricanes-induced liquefaction is closely linked with scour and erosion at/around coastal and marine structures such as offshore wind. The cascading mechanism involving the earthquake-liquefaction-coastal and submarine landslides-tsunamis is highlighted, emphasizing the multi-phased physics of the multi-geohazards. Notably, the critical importance of the dynamics of liquefied gravity flows in coastal and submarine landslides, landslide-induced tsunamis, as well as in high-density turbidity currents is demonstrated, together with the corresponding predictions and observations, in light of their devastating consequences on human lives and critical infrastructures. The paper presents the mitigation concept for a range of submarine geohazards for offshore wind, showing novel submarine geohazards resistant design concepts for bottom-fixed and floating offshore winds for a safe sustainable development across the globe.

Introduction

Submarine geohazards are widespread across the globe and impact people's lives and critical infrastructures. Submarine geohazards range from volcano eruption to earthquakes, tsunamis, seabed liquefaction, seabed creep, submarine slides, turbidity currents, shallow gas eruptions, mud volcanoes, and sediment instability such as migrating bedforms and scour and erosion around marine and offshore structures. Submarine landslide tsunamis are now seen from all geological environments; passive, convergent and transform margins, as well as volcanoes (Tappin and Grilli, 2020; Sassa et al., 2022). Offshore renewable energy systems are rapidly advancing to meet global requirements for sustainable development. Underwater fiber optic cables, underwater power cables, and underwater pipelines have been laid over many parts of the seafloor, and their importance, either strategic and economic, increased dramatically in recent years. However, these marine and offshore infrastructures are at risk from multiple cascading multi-geohazards that include landslides, tsunamis, earthquakes, and volcanic eruptions (Sassa et al., 2022, 2023; Sassa, 2023a). Due to their widespread occurrence across the globe, submarine geohazards are a globally relevant and critical issue to be better addressed in the face of global climate change.

Numerous offshore and coastal geohazards have been recorded on plate subduction zones and the transform plate boundaries, including earthquakes, volcanic eruptions, tsunamis and landslides. For example, the 2002 Stromboli volcanic eruptions induced submarine landslides, causing a tsunami that damaged local infrastructure (Tinti et al., 2005). The submarine landslide off Papua-New Guinea in 1998 caused a tsunami that resulted in 2,200 deaths (Tappin et al., 2001). The Great Alaskan earthquake that took place in Seward and Valdez, Alaska in 1964 induced submarine landslides and tsunamis that caused the loss of more than one hundred lives and properties. The Grand Banks earthquake in 1929 induced submarine landslides, which broke submarine cables over a distance of 1,000 km from its source (Heezen and Ewing, 1952; Whelan, 1994). Recent major events include multiple tsunamis caused by coastal and submarine landslides (Sassa and Takagawa, 2019). Furthermore, seabed soils undergo flows and depositions repeatedly following various events such as storms, earthquakes, sediment transport and gravity flows, making seabed soils susceptible to liquefaction. Case histories, characteristics, and damages of earthquake- or wave-induced seabed liquefaction have been documented by numerous authors (Field et al., 1982; Sassa and Sekiguchi, 1999, 2001; Sumer and Fredsøe, 2002; Sassa et al., 2006; Sumer, 2014; Miyamoto et al., 2020). Resultant damages due to the seabed instability include flotation, settlement, and significant displacement/breakage of pipelines (Christian et al., 1974; Herbich et al., 1984; Damgaard et al., 2006) and subsidence and inclination/failure of offshore and coastal gravity structures (Miyamoto et al., 1989; Sumer, 2014; Sassa et al., 2016). Ongoing and future global climate change is expected to change the severity of wave conditions at the world's coasts (Reguero et al., 2019), which would pose a further risk on offshore renewable energy systems as a consequence of wave-seabed-structure interaction.

This paper concisely summarizes the characteristics, mechanism, prediction and assessment of submarine geohazards with a special emphasis on liquefaction, coastal and submarine landslides, and tsunamis. The mitigation concept for the bottom-fixed and floating offshore wind facilities against such submarine geohazards will then be presented and discussed in light of some recent advances in understanding of the mechanics and physics involved in cascading multi-geohazards.

Submarine Geohazards with a Special Emphasis on Liquefaction, Coastal and Submarine Landslides, and Tsunamis

Earthquake- and severe ocean wave-induced seabed liquefaction, coastal and submarine landslides, high-density gravity flow, and deposition represent large-scale submarine mass movements accompanying the phase change processes during the course of flowage, as shown in Fig. 1. Namely, a gravity flow of liquefied sediment is triggered by significant coastal liquefaction under earthquakes, ocean waves or other environmental forcings, which is followed by the collapse and flow of the liquefied soil under gravity (Fig. 1a). It is categorized as a coastal and submarine landslide that transforms itself into a high-density gravity flow and subsequently flows out over a long distance, leading to re-deposition (Fig. 1b, c). The concurrent processes and the dynamics of liquefied gravity flows are governed by the multi-phased physics (Sassa and Sekiguchi, 2010, 2012; Sassa, 2024). Indeed, pore water migration and associated solidification accompanies the process of flowage leading to redeposition, affecting the dynamics of liquefied gravity flows (Fig. 1). Namely, a solidified region develops in the course of flowage, reestablishing a grain-supported framework. The highly concentrated sediment flows undergo a flow stratification, and the region above the flow surface is effected by turbulence/vortex and entrainment of ambient water, since this region contains only dilute sediment clouds in suspension. Such liquefied gravity flows have a substantial impact on tsunami generation as well as critical infrastructures as described below.

The 2018 Indonesia Sulawesi earthquake and tsunami disasters, which resulted in more than 4,000 fatalities, were cascading disasters that involved the phenomena of liquefaction, landslides, and tsunamis (Sassa and Takagawa 2019). The focal mechanism of the earthquake was strike-slip faulting, being unlikely to produce significant tsunamis, the earthquake in fact caused devastating tsunamis (Sassa and Takagawa, 2019; Carvajal et al., 2019; Polcari et al., 2019; Sepúlveda et al., 2020). The fault length of this M_w=7.5 earthquake was over 150 km. It caused extensive liquefaction and liquefaction-induced flow slides inland where several hundred meters to kilometer scale flow-out distances were observed. Extensive liquefaction and liquefaction-induced flow slides took place not only inland but also along the coast, which resulted in devastating tsunamis (Sassa and Takagawa, 2019).

A notable difference between the 2018 Sulawesi earthquake and the Haiti earthquake (Hornbach et al., 2010), which shared the same basic mechanisms involving a strike-slip fault earthquake, liquefaction, coastal and submarine landslides, and tsunami was such that the liquefaction-induced total collapse and the subsequent flow of coastal land occurred not only at one place, as in the Haiti earthquake. In the 2018 Sulawesi earthquake, the coastal and submarine landslides as characterized by liquefied gravity flows took place at least nine places, simultaneously causing multiple tsunamis throughout the bay and coastal areas (Sassa and Takagawa, 2019), as shown in Fig. 2. Indeed, the spatial area of collapse in the Sulawesi earthquake was ten times greater than that of the Haiti earthquake (Sassa, 2020), whose liquefaction-induced landslide generated the most severe tsunami locally

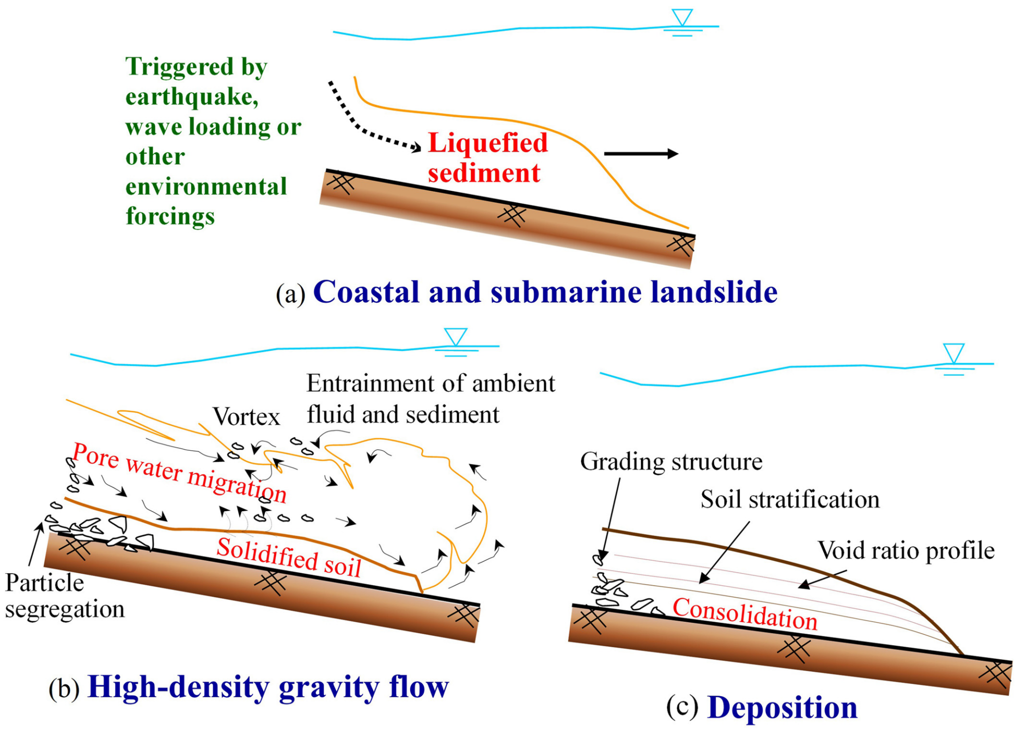

Figure 1. Relevant features of liquefied gravity flows (Sassa and Sekiguchi, 2010, 2012; Sassa, 2024).

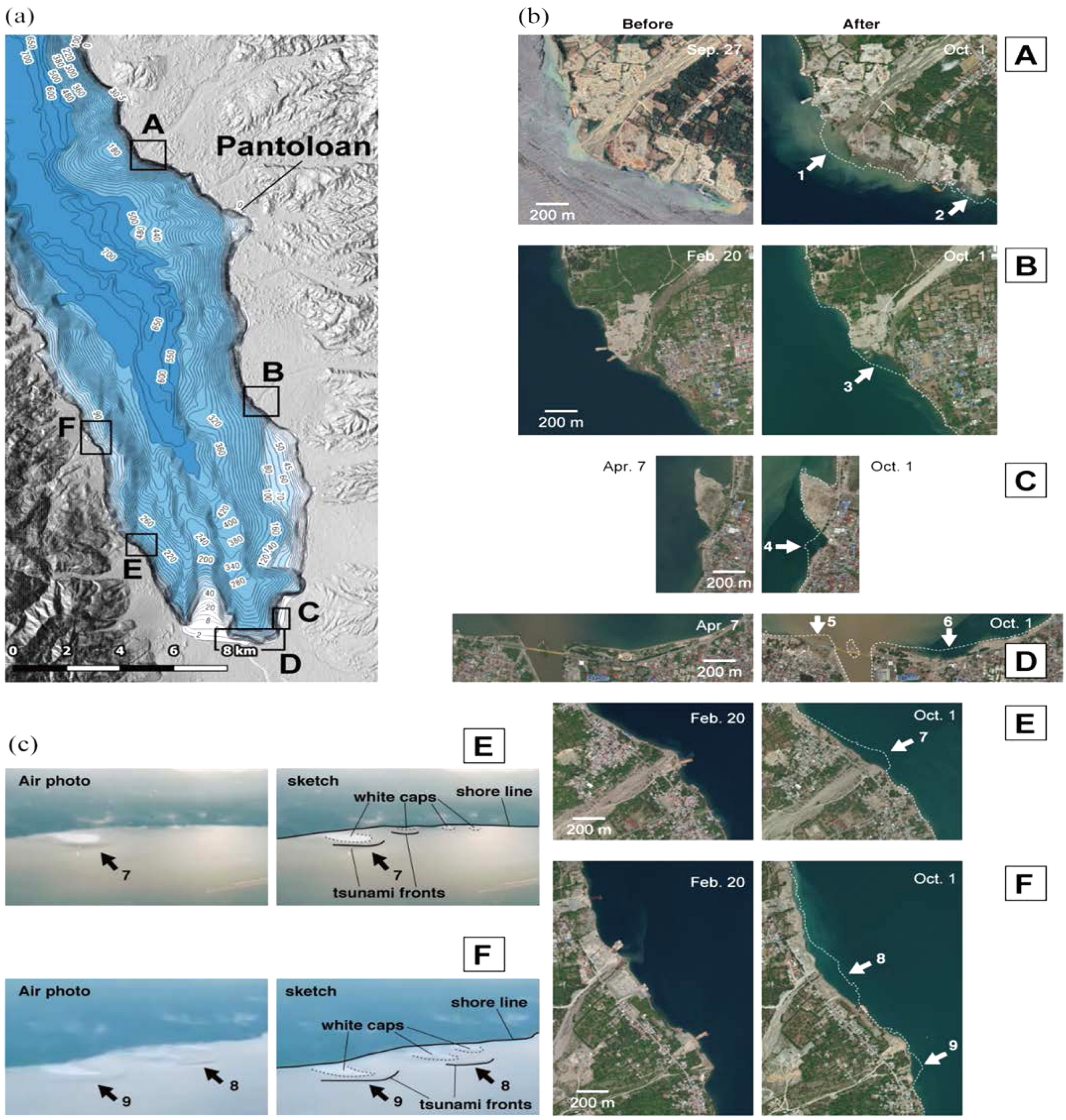

All the locations of the multiple tsunami generations, alongshore distributions and directions conformed to the locations, distributions and directions where the coastal lands collapsed and flowed due to the occurrence of liquefaction.

Figure 2. a Bathymetry of Palu Bay (Badan Informasi Geospasial 2018) and the locations of major coastal retreat (A–F). b Comparisons of satellite images before and after the earthquake (A, Sep. 27: CNES/Airbus 2018; A, Oct. 1 and B–F: Digital Globe Open data Program 2018). Significant coastal retreat areas are indicated by white arrows (No. 1-9). c Aerial photos of multiple tsunami occurrence at the areas E and F, taken just after the earthquake by Mafella (2018). Interpreted sketches are shown aside. The black arrows indicate tsunami fronts and the arrows with numbers 7–9 match those with the same numbers in the satellite images of areas E and F in b. White caps of breaking waves are shown on the land side of the tsunami fronts (Descriptions (blue) added to Fig. 4 in Sassa and Takagawa, 2019).

(Hornbach et al., 2010). Comparing the panels E and F in Fig. 2, all the locations of the multiple tsunami generations, alongshore distributions and directions conformed to the locations, distributions and directions where the coastal lands collapsed and flowed due to the occurrence of liquefaction (Sassa and Takagawa, 2019, Sassa, 2020). Overall, the integrated use of the multiple field evidence, the state-of-the-art knowledge of liquefied gravity flows, and the comparison with a past disaster involving a strike-slip fault earthquake and tsunami, together with the analysis of tidal data (Sassa and Takagawa, 2019) demonstrated that the liquefied gravity flows induced multiple tsunamis, highlighting that both of the 2018 Indonesia Sulawesi earthquake and tsunami disasters stemmed from liquefaction. This not only shows a critical role of the cascading mechanisms involving the earthquake, liquefaction, landslides, and tsunamis, but also indicates the importance of considering liquefaction risks and taking appropriate measures such as relocation, in light of a rational liquefaction prediction and assessment as shown in Sassa and Yamazaki (2017) adopted in practice, for mitigating the impacts of such multi-geohazards in the future.

Large-scale and long-runout liquefied gravity flows caused multiple devastating tsunamis at the 1923 Great Kanto earthquake as well. The results of the analysis of the seafloor dynamics in Sagami Bay before and after the 1923 Great Kanto earthquake (Murata et al., 2024) are shown in Fig. 3. Here, the blue points show deepening areas (outflow) and the red points show shallowing areas (deposition). The blue dotted line represents submarine cable cutting positions (cables broken at six locations) due to a large-scale sediment transport as characterized by the long-runout liquefied gravity flows.

A representative cross-section before and after the earthquake along Line 1 in Fig. 3(a) is shown in Fig. 3(b). The figure indicates an overall landslide over the entire area with the flow thickness up to 142.7 m. The seafloor gradient in the dominant flow area over a 40 km flow-out distance was equal to or less than 0.4°. The bathymetric changes and the associated landslide characteristics showed the widespread long-distance run-out, sharing an important feature of the liquefied

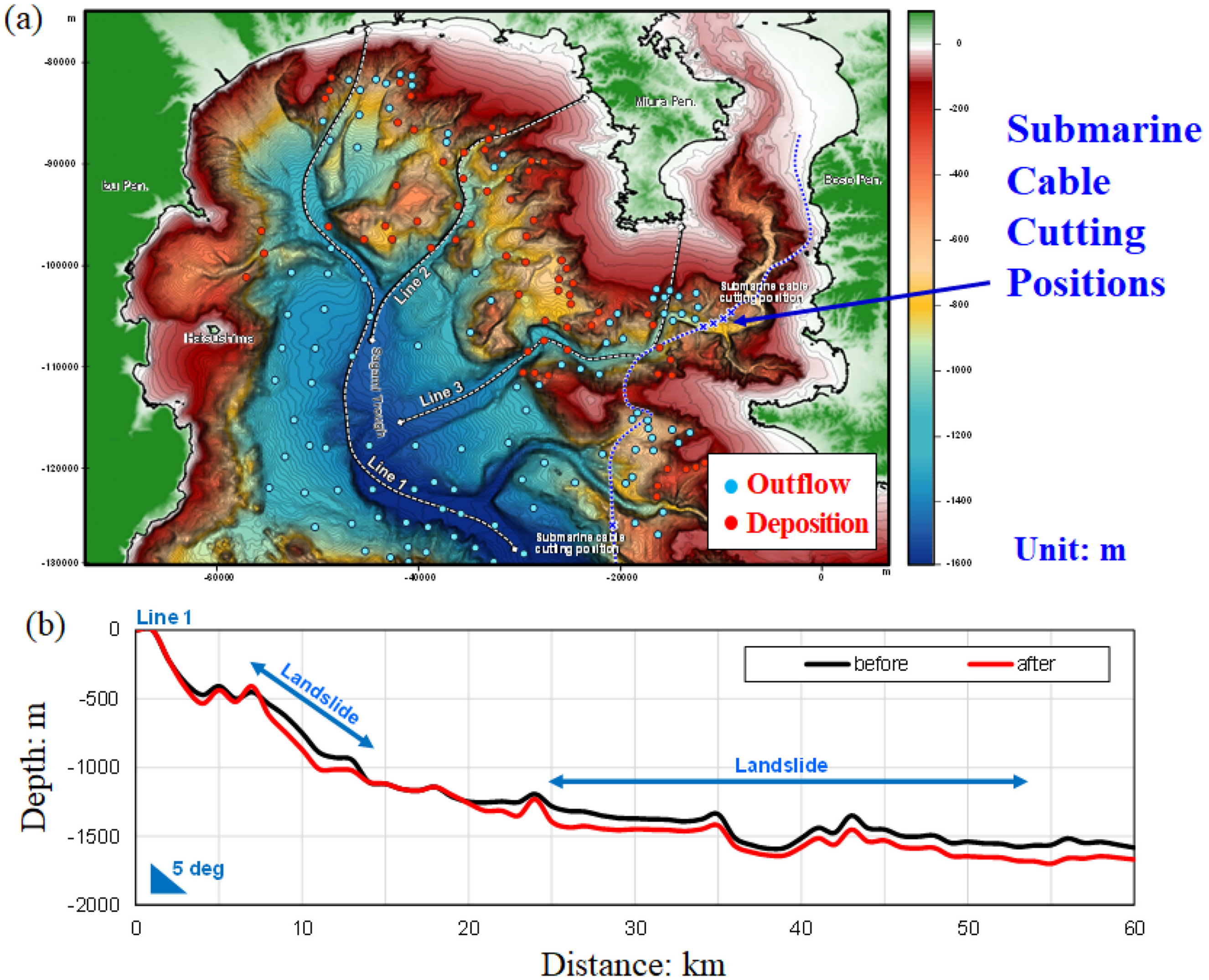

A widespread long-distance run-out shares an important feature of the liquefied gravity flows that can develop over a very gentle slope with less than 1°.

Figure 3. Large-scale long-runout submarine liquefied sediment flows at the 1923 Great Kanto earthquake. (Descriptions (blue) added to Fig. 5a,b in Murata, Ebisuzaki, Sassa et al., 2024).

gravity flows that can develop over a very gentle slope with less than 1º (Field et al., 1982; Sassa and Takagawa, 2019). The dynamics of such submarine liquefied sediment flows features a phase change process in which the transitory fluid-like particulate sediment reestablishes a grain-supported framework accompanying pore fluid migration during flowage (Sassa and Sekiguchi, 2010, 2012). However, the transient high-density liquefied flow has been shown to be characterized by a high-density fluid whose density is equivalent with that of liquefied soil, with the associated theoretical framework showing consistent predictions and agreement with the observed flow behavior from laboratory to field (Sassa and Sekiguchi 2010, 2012).

The results from a range of numerical simulations of the 1923 Great Kanto earthquake tsunamis (Murata et al., 2024) using an optimal fault model with the lowest Residual Sum of Squares (RSS)-values among nine existing models with the observed time-history waveforms, and the submarine landslide tsunami source models due to a high-density liquefied gravity flow based on the theory, experiments, and analysis of field behaviour presented in Sassa et al. (2001), Sassa and Sekiguchi (2010, 2012) and Sassa and Takagawa (2019) are shown in Fig. 4. The results demonstrate that the submarine landslides as represented by a high-density liquefied gravity flow played a pivotal role in consistently accounting for the observed time-history waveforms, the observed initial tsunami motions and their arrival times (Murata et al., 2024), as well as the observed maximum tsunami elevation distributions with more than 12 m tsunami heights along the whole coastal areas in the three Peninsulas involving Izu, Miura and Boso Peninsulas facing Sagami Bay, Tokyo Bay and the Pacific Ocean (Fig. 4). Since a better integrated understanding of the landslide dynamics and multi-phased physics governing landslide tsunami hazard is crucial to reducing the disaster risks of landslides and tsunamis globally (Sassa et al., 2022, 2023), the above liquefaction-induced mechanisms essentially contribute to the global promotion of understanding and reducing the earthquake-induced submarine landslide tsunami risk as cascading multi-geohazards.

The Storegga Slides that took place offshore Norway about 6000 BC caused tsunamis that were recorded all along the coasts of the Greenland-Norwegian Sea (Solheim et al., 2005). The Storegga landslide was one of the largest in the world, with a volume of 2,400–3,200 km^3 (Haflidason et al., 2004), an area of 95,000 km^2, and a runout distance of 300 km (Tappin, 2021; Fig. 5), with the maximum tsunami runups on surrounding coasts exceeding 10m (Bondevik et al., 2003).

Turbidity currents that represent subaqueous density currents driven by the density of suspended sediment typically occur owing to earthquakes, tsunamis, ocean waves, or other environmental forcings (Bouma et al., 1985; Hsu et al., 2008; Breien et al., 2010; Arai et al., 2013; Talling et al., 2013; Pope et al., 2017; Paull et al., 2018; Sequeiros et al., 2019). Accordingly, turbidity currents are closely linked to the occurrence of liquefaction and liquefied flows (Breien et al., 2010; Paull et al., 2018; Sequeiros et al., 2019). In fact, powerful high-density and long-travelling turbidity currents (Paull et al., 2018) share some essential features with those of liquefied gravity flows, with reference to Fig. 1 (Sassa and Sekiguchi, 2010, 2012). Disasters caused by such turbidity currents include cable breaks, rupture and pipeline damage. For instance, a total of eleven telecommunication cables broke due to two major Pingtung earthquakes (M_w7)-induced submarine landslides and turbidity currents offshore Taiwan (Hsu et al., 2008). A 25 years' analysis of a global database of fiber-optic cable breaks and associated submarine mass movements indicates that all Mw 9.0 earthquakes triggered mass flows and turbidity currents without exceptions (Pope et al., 2017). Typhoons/Cyclones/Hurricanes-induced severe ocean waves can cause liquefaction that brings about large-scale turbidity currents, impacting critical infrastructures such as pipelines (Sequeiros et al., 2019). Hence, liquefaction, coastal and submarine landslides, turbidity currents, and tsunamis are the important cascading multi-geohazards against which the mitigation concept becomes vitally important for sustainable development worldwide.

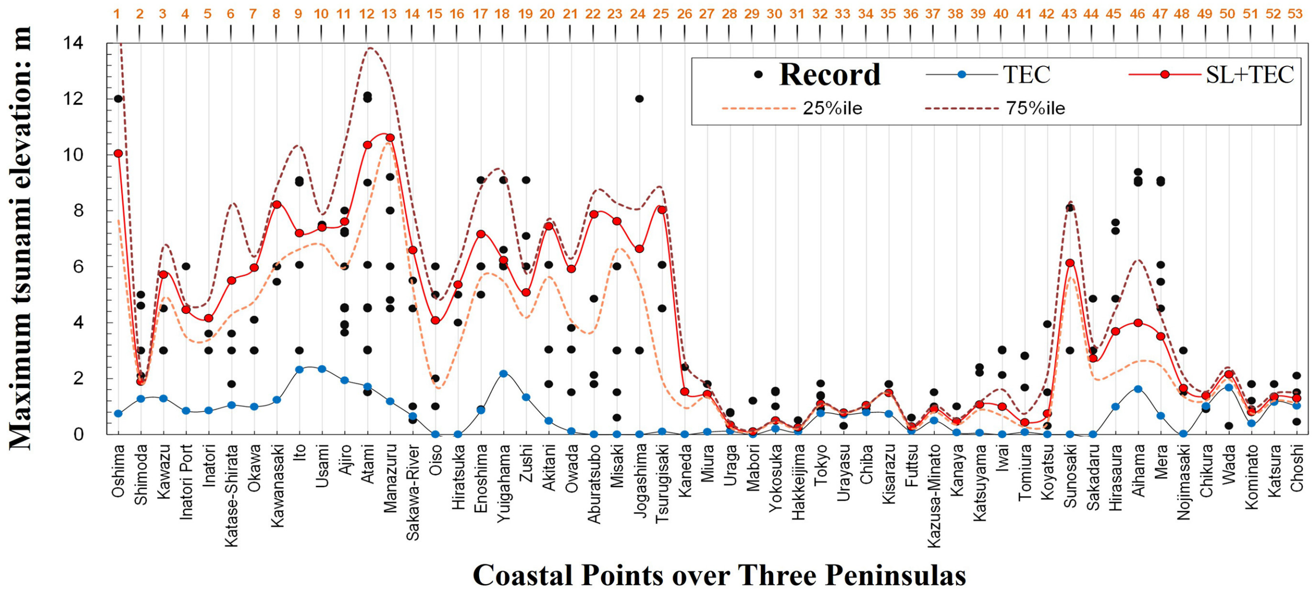

Figure 4. Submarine landslides as represented by a high-density liquefied gravity flow-induced tsunamis: predictions and observations along three peninsulas involving Izu, Miura, and Boso Peninsulas facing Sagami Bay, Tokyo Bay, and the Pacific Ocean, adopted from Fig. 9a in Murata, Ebisuzaki, Sassa et al. (2024).

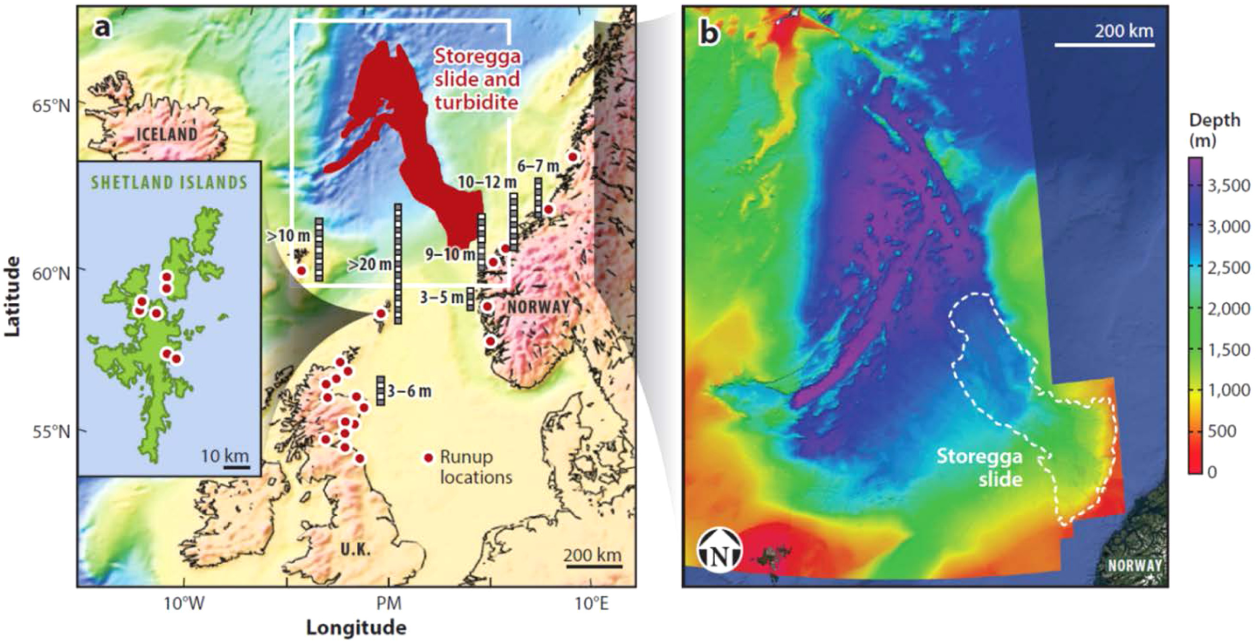

The Storegga landslide was one of the largest in the world, with a runout distance of 300 km and the maximum tsunami runups on surrounding coasts exceeding 10m.

Figure 5. The Storegga, Norway, landslide and tsunami. Panel a shows landslide location and elevation of tsunami runups on surrounding coasts, adapted from Bondevik et al. (2003). Panel b shows a digital elevation model of the landslide (white dotted line) and the resulting turbidite covering the purple seabed region to the northwest. Figure adapted from EMODnet Bathymetry Consort. (2018). (Descriptions (blue) added to Fig. 7 in Tappin 2021).

Mitigation Concept for Offshore Wind

The offshore renewable energy systems are subjected to diverse forms of submarine geohazard risks, such as seabed liquefaction induced by earthquakes and ocean waves and associated large-scale mass movements. Amid global climate change, the ocean wave conditions are becoming more severe along the world's coasts (Reguero et al., 2019). This fact makes floating offshore wind facilities that are installed in relatively deep waters compared with the bottom-fixed offshore wind facilities more susceptible to liquefaction under both earthquakes and severe ocean waves.

In light of some recent advances in understanding of the mechanics and physics of a range of cascading submarine geohazards pertaining to liquefaction, novel mitigation concepts for bottom-fixed and floating offshore winds are presented below. Specifically, the former addresses the stability and the countermeasure concept for the monopiles, suction buckets, and jacket-type foundations for the bottom-fixed offshore wind facilities, whereas the latter addresses the stability and the preventive maintenance concept for the anchors and cables for the floating offshore wind facilities.

Wave-Induced Liquefaction-Scour Countermeasure Concept for Bottom-Fixed Offshore Wind

Wave-induced seabed instability considerably affects the stability of coastal and offshore structures resting on/in the seabed. Representative forms and processes of the instability involve scour and seabed liquefaction. Indeed, scour and wave-induced liquefaction are physically interconnected, simultaneously affecting the stability of structures (Sassa, 2021).

Wave-seabed-monopile interaction has been studied by a prototype-scale-stress testing, namely, centrifuge wave testing, where the relevant scaling laws for wave-induced seabed liquefaction, i.e. time-scaling laws for fluid wave propagation and soil consolidation as well as for foundation scour were satisfied (Miyamoto et al., 2021). The results demonstrate that the monopile started significant structural rocking when liquefaction occurred and the residual displacement of the pile increased markedly with the downward progress of the liquefied zone, eventually leading to the collapse of the pile.

The wave-induced liquefaction-scour countermeasure concept for offshore monopile foundations is shown in Fig. 6. Here, in a usual scour protection around a pier or monopile in the context of wave-seabed-structure interaction, the extent of the scour protection is 3 to 4 times the diameter D of the monopile (Sumer and Fredsøe, 2002). The results shown in Fig. 6 demonstrate that scour protection increased the liquefaction resistance depending on the diameter ratios of the scour protection and the pile, however, it could not prevent the collapse of the monopile once liquefaction occurred (Miyamoto et al., 2021). These results indicate the importance of soil stratification on the wave-seabed-structure interactions. Hence, wave-induced seabed liquefaction needs to be considered in a rational design of coastal structures such as offshore wind monopile foundations. Namely, once liquefaction is predicted to occur under design waves (Sassa et al., 2026), the scour protection area can be determined so that the increased liquefac-

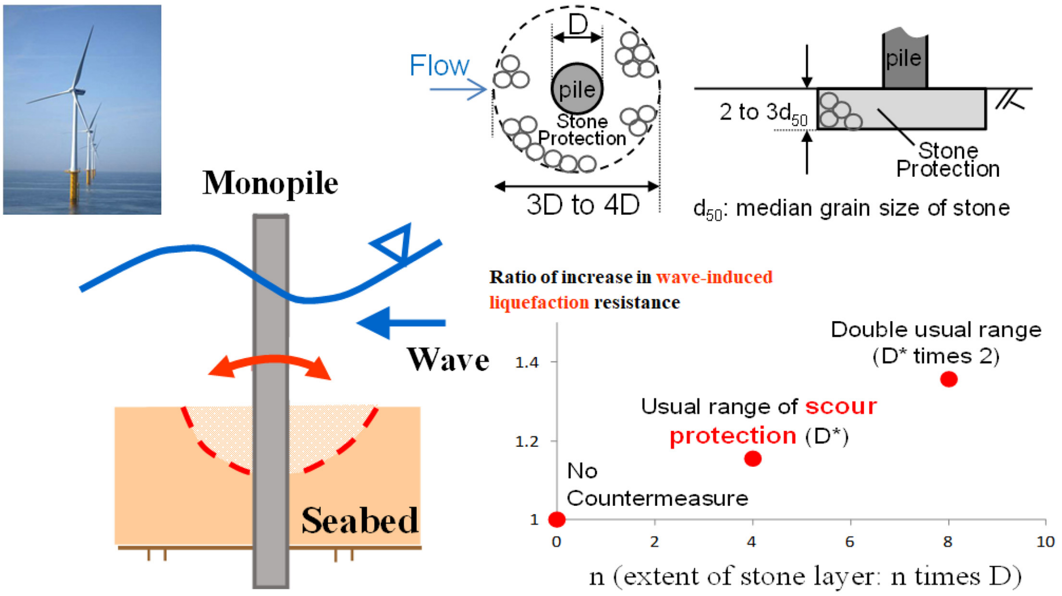

Figure 6. Wave-Seabed-Structure Interaction: wave-induced liquefaction-scour countermeasure concept for offshore monopile foundations. (Sassa 2023b, 2024).

tion resistance may prevent the occurrence of liquefaction under the severe wave conditions, thereby suppressing and mitigating the impact of the seabed liquefaction and its consequences. This migration concept can be utilized for another type of the bottom-fixed offshore wind foundations such as suction bucket foundations whose stability is closely linked with wave-induced seabed liquefaction and its spread (Miyamoto et al., 2023).

The filter layer installation in the form of rock scour protection has

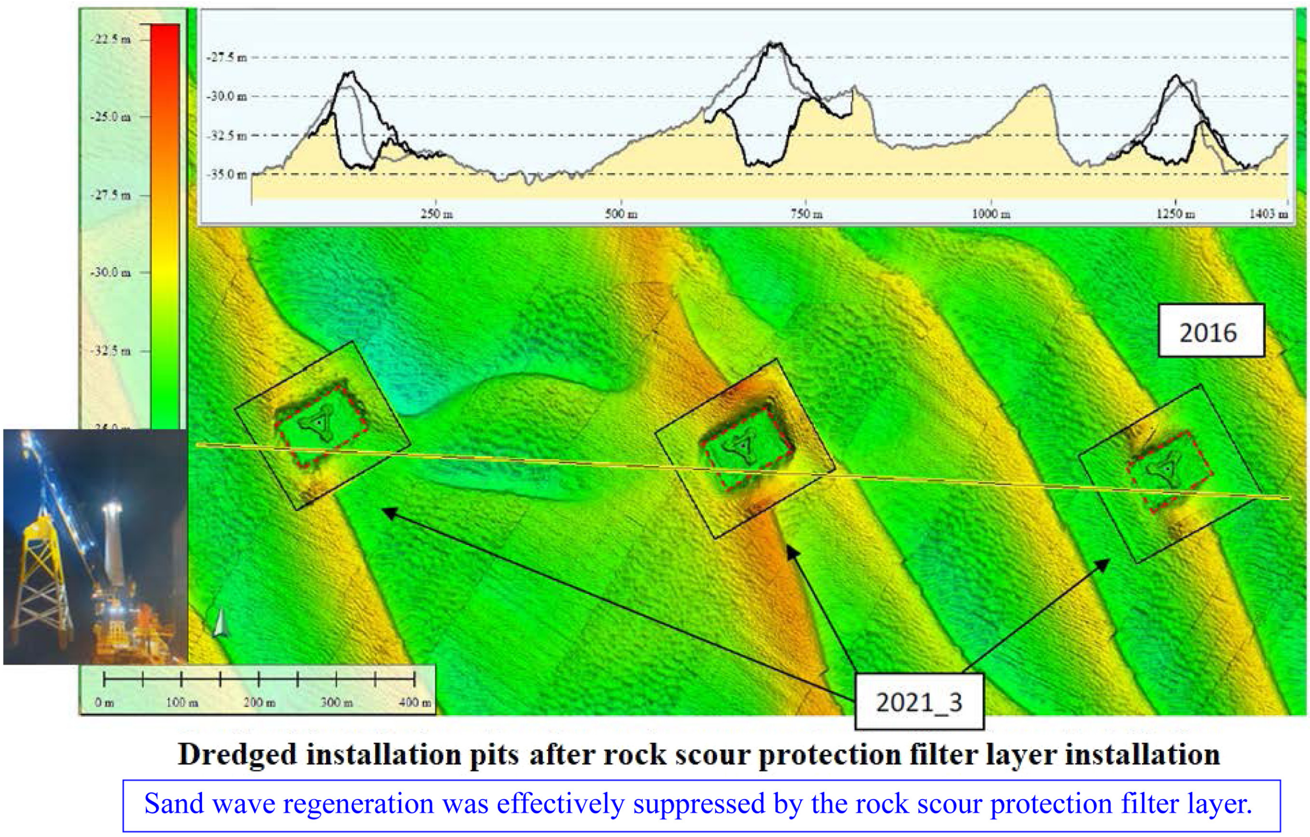

Figure 7. Performance of rock scour protection filter layer installation in 2016 (grey) and 2021 (black) (Descriptions (blue) added to Figure 4 top panel in Roulund et al., 2023).

also been shown to be effective in suppressing the damage of scour around jacket-type offshore wind foundations (Roulund et al., 2023), as shown in Fig. 7. Here, the grey and black lines denote the bathymetric changes observed in 2016 and 2021, respectively, following the filter layer installation. The results show that the sand wave regeneration was effectively suppressed by the rock scour protection filter layer.

Submarine Landslide Flow Impact Assessment and Preventive Maintenance

Submarine liquefied sediment flows can have a substantial impact on diverse offshore wind structure foundations. The influence of the submarine landslide and liquefied flow on such structure foundations may be characterized by a high-density fluid corresponding to the mass density of the flowing landslide body, namely that of the in-situ liquefied seabed (Makino et al., 2025). This means that by comparing the maximum impact force considering the in-situ liquefied ground density and the design resistant force of the facility, one could set a preventive maintenance against the corresponding submarine landslide/liquefied flow in the future. Further, the impact pressure exerted on coastal and offshore structures has been found to be twice or higher than the pressure acting on the seabed surface (Makino et al., 2025). This means that one may substantially reduce the impact and influence of such submarine landslide flows depending on the embedded area of the structures.

Submarine Geohazards Resistant Design Concept for Anchors and Cables of Floating Offshore Wind

Based on the state-of-the-art understanding of the seabed liquefaction-induced impact on coastal and offshore infrastructures, which stems from the evidences from laboratory to field settings, including both observations and theoretical/numerical analyses (Sassa, 2023b; Sassa et al., 2026), this section presents a novel submarine geohazards-resistant design concept for anchors and cables of floating offshore wind (Sassa, 2024). Seabed liquefaction governs the fate of floating or sinking of a structure resting on/in the seabed. Namely, under conditions where the overall density of a structure is lower than the mass density of a liquefied seabed ground, the structure floats up, whereas under conditions where the overall density of a structure is higher than the mass density of a liquefied seabed ground, the structure sinks into the liquefied seabed. In the case of the latter, the structure may settle into the seabed ground in association with the liquefaction, scour and sediment transport. A range of the field and experimental evidence show that pipeline floatation is closely linked with the seabed liquefaction. Indeed, the sinking and flotation of a pipeline and a cable is controlled by the relationship between the overall density of a structure and the mass density of a liquefied soil (Sassa, 2024). The corresponding structure-liquefied soil density ratio equal to unity serves as an index value below which floating takes place and above which sinking ensues.

The standard anchor types for floating offshore wind are drug anchors, pile anchors, suction anchors, and gravity anchors, and the typical mooring systems are catenary systems, taut systems, tension-leg systems, as shown in Fig. 8. Depending on the mooring systems, there exist the vertical tension forces at ordinary times, as denoted by T_v in Fig. 8. By defining the anchor mass density by ρ_A, the anchor volume by V_A, and the mass density of liquefied soil by ρ_L, the anchor behaviour during seabed liquefaction can be classified as "Sinking", "Floating", and "Stable" depending on the three conditions denoted in Fig. 8. For each anchor behaviour, under conditions where $T_v = 0$ and $T_v \neq 0$, one can realize the submarine geohazards resistant anchors by setting and selecting anchors and mooring systems that take into account of the states and relationships shown in Fig. 9. Importantly, under conditions where the anchor behaviour is "stable", the stability of a floating offshore wind can be kept continuously during seabed liquefaction by preventing floatation, burial and settlement of the anchors while keeping essentially the same depth in the ground (Sassa, 2024). This also ensures a higher horizontally-moving resistance force for the anchors owing to the higher mass density of the liquefied seabed ground than the ambient fluid, thereby reducing the impact from submarine landslides and flows.

By defining the cable mass density by ρ_C and the mass density of

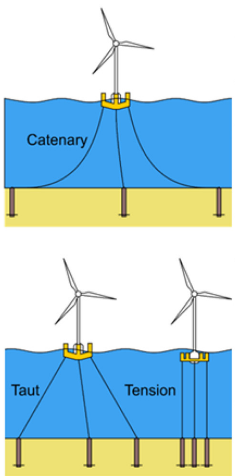

Mooring System
(European Commission)

Anchor type	
Drag anchor, Pile anchor, Suction anchor, Gravity anchor	
Mooring system	
Catenary system, Taut system, Tension-leg system	
Vertical tension force at ordinaty times T_V	
Absent, Present, Present	
Anchor mass density, Anchor volume, Mass density of liquefied soil	
ρ_A, V_A, ρ_L	
Anchor behaviour during seabed liquefaction	
Under conditions where $(\rho_A - \rho_L) g V_A - T_V > 0$,	「**Sinking**」
Under conditions where $(\rho_A - \rho_L) g V_A - T_V < 0$,	「**Floating**」
Under conditions where $(\rho_A - \rho_L) g V_A - T_V \cong 0$,	「**Stable**」

Figure 8. Anchor behaviour during seabed liquefaction (Sassa, 2024).

Anchor behaviour during seabed liquefaction		Submarine Geohazards Resistant Design Concept for Anchors
Under conditions where $(\rho_A - \rho_L) gV_A - T_V > 0$ 「Sinking」	⇨	When $T_V = 0$: Set/Select Anchors where $(\rho_A - \rho_L)$ becomes small. When $T_V \neq 0$: Set/Select anchors and mooring systems where $(\rho_A - \rho_L) g V_A / T_V$ approaches unity
Under conditions where $(\rho_A - \rho_L) gV_A - T_V < 0$ 「Floating」	⇨	When $T_V = 0$: Set/Select Anchors where $(\rho_L - \rho_A)$ becomes small. When $T_V \neq 0$: Set/Select anchors and mooring systems where $(\rho_A - \rho_L) g V_A / T_V$ approaches unity
Under conditions where $(\rho_A - \rho_L) gV_A - T_V \cong 0$ 「Stable」	⇨	The stability of the floating offshore wind can be kept continuously during seabed liquefaction by preventing floatation, burial and sinking of anchors while keeping essentially the same depth in the seabed ground.

Under conditions where part of the anchor is exposed, defining the anchor volume below the seabed surface by V_B, 「$(\rho_A - \rho_L) gV_A$」 is replaced by 「$\rho_A gV_A - \rho_L gV_B - \rho_w g(V_A - V_B)$」, and when $Tv = 0$, 「$(\rho_A - \rho_L)$」 is replaced by 「$\rho_A - \rho_L V_B/V_A - \rho_w(1 - V_B/V_A)$」.

Figure 9. Submarine geohazards resistant design concept for anchors of floating offshore wind (Sassa, 2024).

Cable mass density, Mass density of liquefied soil: ρ_C, ρ_L — Cable behaviour during seabed liquefaction		Submarine Geohazards Resistant Design Concept for Cables
Under conditions where $\rho_C > \rho_L$ 「Sinking」	⇨	Preventive maintenance/countermeasures for settlement
Under conditions where $\rho_C < \rho_L$ 「Floating」	⇨	Preventive maintenace/countermeasures for floatation
Under conditions where $\rho_C \cong \rho_L$ 「Stable」	⇨	The stability of the floating offshore wind can be kept continuously during seabed liquefaction by preventing floatation, burial and sinking of cables while keeping essentially the same depth in the seabed ground.

Figure 10. Submarine geohazards resistant design concept for cables of floating offshore wind (Sassa, 2024).

liquefied soil by ρ_L, the cable behaviour during seabed liquefaction can be classified as "Sinking", "Floating", and "Stable" depending on the three conditions denoted in Fig. 10. For each cable behaviour, one can realize the submarine geohazards resistant cables by adopting the preventive maintenance and countermeasures for settlement under conditions where "Sinking" ensues, and by adopting the preventive maintenance and countermeasures for floatation under conditions where "Floating" ensues, as shown in Fig. 10. Importantly, under conditions where the cable behaviour is "Stable", the stability of a floating offshore wind can be kept continuously during seabed liquefaction by preventing floatation, burial and settlement of the cables while keeping essentially the same depth in the ground (Sassa, 2024). This also ensures a higher horizontally-moving resistance force for the cables owing to the higher mass density of the liquefied seabed ground than the ambient fluid, thereby reducing the impact from submarine landslides and flows. At/around the boundaries between "Stable", "Sinking" and "Floating" regions, the cables are particularly susceptible to the submarine geohazard risks and accordingly, the above preventive maintenance/countermeasure concept becomes vitally important amid climate change.

Summary

This paper has concisely summarized the characteristics, mechanism, prediction and assessment of submarine geohazards with a special emphasis on liquefaction, coastal and submarine landslides, and tsunamis. It has shown the cascading mechanisms involving the earthquake-liquefaction-coastal and submarine landslides-tsunamis, emphasizing the multi-phased physics of the multi-geohazards. Notably, the critical importance of the liquefied gravity flows in coastal and submarine landslides, landslide-induced tsunamis, as well as in the high-density turbidity currents has been demonstrated, together with the corresponding predictions and observations, in the light of their devastating consequences on human lives and critical infrastructures. Based on the state-of-the-art understanding of the seabed liquefaction-induced impact on coastal and offshore infrastructures, the paper has also presented and discussed the mitigation concept for a range of cascading multi-geohazards pertaining to liquefaction under both earthquakes and severe ocean waves, showing novel submarine geohazards resistant design concepts for the bottom-fixed and floating offshore wind facilities for a safe sustainable development worldwide.

References

Arai, K., Naruse, H., Miura, R., Kawamura, K., Hino, R., Ito, Y., Inazu, D., Yokokawa, M., Izumi, N., Murayama, M., and Kasaya, T., 2013, Tsunami-generated turbidity current of the 2011 Tohoku-Oki earthquake. Geology, v. 41, pp. 1195–1198. doi:10.1130/G34777.1

Badan Informasi Geospasial, 2018, Contour map of Palu Bay, Retrieved from https://cloud.big.go.id [accessed 30th October 2018].

Bondevik, S., Mangerud, J., Dawson, S., Dawson, A., and Lohne, O., 2003, Record-breaking height for 8000-year-old tsunami in the North Atlantic. Eos Trans, AGU, v. 84, pp. 289–293.

Bouma, A.H., Normark, W.R., and Barnes, N.E., 1985, Submarine Fans and Related Turbidite Systems. Springer, New York.

Breien, H., Blasio, F.V., Elverhoi, A., Nystuen, J.P., and Harbitz, C.B., 2010, Transport mechanisms of sand in deep-marine environments-Insights based on laboratory experiments. Journal of Sedimentary Research, v. 80, pp. 975–990. doi:10.2110/jsr.2010.079

Carvajal, M., Araya-Cornejo., C., Sepulveda, I., Melnick, D., and Haase, J.S., 2019, Nearly Instantaneous Tsunamis Following the *Mw* 7.5 2018 Palu Earthquake. Geophysical Research Letters, v. 46. doi:10.1029/2019GL082578

Christian, J.T., Taylor, P.K., Yen, J.K.C., and Erali, D.R., 1974, Large diameter underwater pipeline for nuclear power plant designed against soil liquefaction. In Proc., Offshore Technology Conf., pp. 597–606. Houstan: Offshore Technology Conference.

Damgaard, J.S., Sumer, B.M., Teh, T.C., Palmer, A.C., Foray, P., and Osorio, D., 2006, Guidelines for pipeline on-bottom stability on liquefied noncohesive seabeds. Journal of Waterway, Port, Coastal, and Ocean Engineering, v. 132, pp. 300–309.

Digital Globe Open data Program, 2018, Satellite Images of Palu and Donggala, Sulawesi, Indonesia, Retrieved from https://www.digitalglobe.com/opendata/indonesia-earthquake-tsunami/ [accessed 30th October 2018].

Field, M.E., Gardner, J.V., Jennings, A.E., and Edwards, E.D., 1982, Earthquake-induced sediment failures on a 0.25° slope, Klamath River delta, California. Geology, v. 10, pp. 542–546. doi:10.1130/0091-7613(1982)10%3C542:ESFOAS%3E2.0.CO;2

Haeussler, P., Lee, H., Ryan, H.F., Labay, K., Kayen, R.E., Hampton, M.A., and Suleimani. E., 2008, Submarine Landslides and Tsunamis at Seward and Valdez Triggered by the 1964 Magnitude 9.2 Alaska Earthquake. Alaska Geology, Newsletter of the Alaska Geological Society, v. 39, pp. 1–2.

Haflidason, H., Sejrup, H.P., Nygard, A., Mienert, J., Bryn, P., Lien, R., Forsberg, C.F., Berg, K., and Masson, D., 2004, The Storegga Slide: architecture, geometry and slide development. Mar. Geol., v. 213, pp. 201–234.

Heezen, B.C., and Ewing, M., 1952, Turbidity currents and submarine slumps and the 1929 Grand Banks earthquake. American Journal of Science, v. 250, pp. 849–873.

Herbich, J.B., Schiller, R.E., Watanabe, R.K., and Dunlop, W.A., 1984, Seafloor Scour: Design Guidelines for Ocean-founded Structures. Marcel Dekker, New York.

Hornbach, M.J., Braudy, N., Briggs, R.W., Cormier, M.H., Davis, M.B., Diebold, J.B., Dieudonne, N., Douilly, R., Frohlich, C., Gulick, S.P.S., Johnson, H.E., Mann, P., McHugh, C., Ryan-Mishkin, K., Prentice, C.S., Seeber, L., Sorlien, C.C., Steckler, M.S., Symithe, S.J., Taylor, F.W., and Templeton, J. 2010, High tsunami frequency as a result of combined strike-slip faulting and coastal landslides. Nature Geoscience, v. 3, pp. 783–788. doi:10.1038/ngeo975

Hsu, S.K., Kuo, J., Lo, C.L., Tsai, C.H., Doo, W.B., Ku, C.Y., and Sibuet, J.C., 2008, Turbidity Currents, Submarine Landslides and the 2006 Pingtung Earthquake off SW Taiwan. Terrestrial, Atmospheric and Oceanic Sciences, v. 19, pp. 767–772.

Mafella, R., 2018, Batik Air ID 6231 scheduled to depart at 17.55, door closed at 17.52 then pushed back. 18.02 after cleared for takeoff, tower building collapsed. [Instagram Post], Retrieved from https://www.instagram.com/p/BoRttnsn5po/?taken-by=icoze_ricochet [accessed 30th October 2018].

Makino, R., Miyamoto J., Sassa, S., and Tsujino, G., 2025, Centrifuge experiments on submarine gravity flow of liquefied sand and its impact on structures. Proceedings of the 12th International Conference on Scour and Erosion. Online Library of ISSMGE.

Miyamoto, T., Yoshinaga, S., Soga, F., Shimizu, K., Kawamata, R., and Sato, M., 1989, Seismic prospecting method applied to the detection of offshore breakwater units settling in the seabed. Coast. Coastal Engineering in Japan, v. 32, pp. 103–112.

Miyamoto, J., Sassa, S., Turugasaki, K., and Sumida, H., 2020, Wave-induced liquefaction and floatation of a pipeline in a drum centrifuge. Journal of Waterway, Port, Coastal, and Ocean Engineering, v. 146, 04019039.

Miyamoto, J., Sassa, S., Tsurugasaki, K., and Sumida, H., 2021, Wave-induced liquefaction and instability of offshore monopile in a drum centrifuge. Soils Found. v. 61, pp. 35–49. doi:10.1016/j.sandf.2020.10.005

Miyamoto, J., Sassa, S., Tsurugasaki, K., and Sumida, H., 2023, Wave-Induced Liquefaction and Stability of Suction Bucket Foundation in Drum Centrifuge. Journal of Geotechnical and Geoenvironmental Engineering, v. 149, 04023013. doi:10.1061/JGGEFK.GTENG-11247

Murata, K., Ebisuzaki, T., Sassa, S., Takagawa, T., Masuda, K., Miyamoto, T., Ohno, M., and Maruyama, S., 2024, Submarine landslides and tsunami genesis in Sagami Bay, Japan, caused by the 1923 Great Kanto earthquake. Landslides, v. 21, pp. 1811–1827. doi:10.1007/s10346-024-02231-x

Paull, C.K., Talling, P.J., Maier, K.L., Parsons, D., Xu, J., Caress, D.W., Gwiazda, R., Lundsten, E.M., Anderson, K., Barry, J.P., Chaffey, M., O'Reilly, T., Rosenberger, K.J., Gales, J.A., Kieft, B., McGann, M., Simmons, S.M., McCann, M., Sumner, E.J., Clare, M.A., and Cartigny, M.J., 2018, Powerful turbidity current driven by dense basal layers. Nature Communications, v. 9, 4114. doi:10.1038/s41467-018-06254-6

Polcari, M., Tolomei, C., Bignami, C., and Stramondo, S., 2019, SAR and Optical Data Comparison for Detecting Co-Seismic Slip and Induced Phenomena during the 2018 M_w 7.5 Sulawesi Earthquake. Sensors, v. 19, 3976. doi:10.3390/s19183976

Pope, E.L., Talling, P.J., and Carter, L., 2017, Which earthquakes trigger damaging 959 submarine mass movements: Insights from a global record of submarine cable breaks?. Marine Geology, v. 384, pp. 131–146. doi:10.1016/j.margeo.2016.01.009

Reguero, B.G., Losada, I.J., and Méndez, F.J., 2019, A recent increase in global wave power as a consequence of oceanic warming. Nature Communications, v. 10, 205. doi:10.1038/s41467-018-08066-0

Roulund, A., Riezebos, H.J., and Saverymuttu, K., 2023, Foundation installation in sandwave fields: Field observations of sandwave regeneration and sediment infill. Proceedings of the 11th International Conference on Scour and Erosion, pp. 1–16. Online Library of ISSMGE

Sassa, S., and Sekiguchi, H., 1999, Wave-induced liquefaction of beds of sand in a centrifuge. Géotechnique, v. 49, pp. 621–638. doi:10.1680/geot.1999.49.5.621

Sassa, S., and Sekiguchi, H., 2001, Analysis of wave-induced liquefaction of sand beds. Géotechnique, v. 51, pp. 115–126. doi:10.1680/geot.2001.51.2.115

Sassa, S., Sekiguchi, H., and Miyamoto, J., 2001, Analysis of progressive liquefaction as a moving-boundary problem. Géotechnique, v. 51, pp. 847–857. doi:10.1680/geot.2001.51.10.847

Sassa, S., Takayama, T., Mizutani, M., and Tsujio, D., 2006, Field observations of the build-up and dissipation of residual pore pressures in seabed sands under the passage of storm waves. Journal of Coastal Research, v. 39 (Special Issue), pp. 410–414.

Sassa, S., and Sekiguchi, H., 2010, LIQSEDFLOW: Role of two-phase physics in subaqueous sediment gravity flows. Soils Found., v. 50, pp. 495–504. doi:10.3208/sandf.50.495

Sassa, S., and Sekiguchi, H., 2012, Dynamics of Submarine Liquefied Sediment Flows: Theory, Experiments and Analysis of Field Behavior. Advances in Natural and Technological Hazards Research, v. 31, pp. 405–416. doi:10.1007/978-94-007-2162-3_36

Sassa, S., Takahashi, H., Morikawa, Y., and Takano, D., 2016, Effect of overflow and seepage coupling on tsunami-induced instability of caisson breakwaters. Coastal Engineering, v. 117, pp. 157–165. doi:10.1016/j.coastaleng.2016.08.004

Sassa, S., and Yamazaki, H., 2017, Simplified liquefaction prediction and assessment method considering waveforms and durations of earthquakes. Journal of Geotechnical and Geoenvironmental Engineering, v. 143, 04016091. doi:10.1061/(ASCE)GT.1943-5606.0001597

Sassa, S., and Takagawa, T., 2019, Liquefied gravity flow-induced tsunami: first evidence and comparison from the 2018 Indonesia Sulawesi earthquake and tsunami disasters. Landslides, v. 16, pp. 195–200. doi:10.1007/s10346-018-1114-x

Sassa, S., 2020, Cascading Mechanisms Behind the 2018 Indonesia Sulawesi Earthquake and Tsunami Disasters: Inland/Coastal Liquefaction, Landslides and Tsunami. Keynote Paper. Springer Series in Geomechanics and Geoengineering. doi:10.1007/978-3-030-46351-9_4

Sassa, S., 2021, Mechanics and Countermeasures of Scour and Internal Erosion: Tsunami/Wave-Seabed-Structure Interaction. Lecture Notes in Civil Engineering, v. 177, Keynote paper. doi:10.1007/978-981-16-4783-3_1

Sassa, S., Grilli, S.T., Tappin, D.R., Sassa, K., Karnawati, D., Gusiakov, V.K., and Løvholt, F., 2022, Understanding and reducing the disaster risk of landslide-induced tsunamis: a short summary of the panel discussion in the World Tsunami Awareness Day Special Event of the Fifth World Landslide Forum. Landslides, v. 19, pp. 533–535. doi:10.1007/s10346-021-01819-x

Sassa, S., Grilli, S.T., Tappin, D.R., Sassa, K., Karnawati, D., Gusiakov, V.K., and Løvholt, F., 2023, Understanding and reducing the disaster risk of landslide-induced tsunamis: outcome of the panel discussion and the World Tsunami Awareness Day Special Event of the Fifth World Landslide Forum. Progress in Landslide Research and Technology, v. 1, pp. 65–81. doi:10.1007/978-3-031-16898-7_4

Sassa, S., 2023a, Landslides and Tsunamis: Multi-Geohazards. Landslides, v. 20, pp. 1335–1341. doi:10.1007/s10346-023-02084-w

Sassa, S., 2023b, Recent Advances in the Mechanics and Countermeasures of Scour and Erosion. Opening Keynote Speech for the 11th International Conference on Scour and Erosion (ICSE-11), ISSMGE.

Sassa, S., 2024, Submarine Geohazards Resistant Design Concept for Anchors and Cables of Floating Offshore Wind. Keynote Speech for the 37th International Geological Congress 2024.

Sassa, S., Naruse, H., and Tappin, D., 2026, Recent Advances in Understanding and Reducing Multi-Geohazard Risks: Liquefaction, Coastal and Submarine Landslides, Turbidity Currents, and Tsunamis. Progress in Landslide Research and Technology, v. 4.

Sepúlveda, I., Haase, J.S., Carvajal, M., Xu, X., and Liu, P.L., 2020, Modeling the sources of the 2018 Palu, Indonesia, tsunami using videos from social media. Journal of Geophysical Research-Solid Earth, v. 125, e2019JB018675. doi:10.1029/2019JB018675

Sequeiros, O.E., Pittaluga, M.B., Frascati, A., Pirmez, C., Masson, D.G., Weaver, P., Crosby, A.R., Lazzaro, G., Botter, G., and Rimmer, J.G., 2019, How typhoons trigger turbidity currents in submarine canyons. Scientific Reports, v. 9, 9220. doi:10.1038/s41598-019-45615-z

Solheim, A., Bryn, P.B., Sejrup, H.P., Mienert, J., and Berg, K., 2005, Ormen Lange-an integrated study for safe development of a deep-water gas field within the Storegga Slide Complex, NE Atlantic continental margin; executive summary. Marine and Petroleum Geology, v. 22, pp. 1–9.

Talling, P.J., Paull, C.K., and Piper, D.J.W., 2013, How are subaqueous sediment density flows triggered, what is their internal structure and how does it evolve? Direct observations from monitoring of active flows. Earth-Science Reviews, v. 125, pp. 244–287. doi:10.1016/j.earscirev.2013.07.005

Sumer, B.M., and Fredsøe, J., 2002, The mechanics of scour in the marine environment. Advanced Series on Ocean Engineering, v. 17.

Sumer, B.M., 2014, Liquefaction around marine structures. Advanced Series on Ocean Engineering, v. 39, World Scientific.

Tappin, D.R., Watts, P., McMurtry, G.M., Lafoy, Y., and Matsumoto, T., 2001, The Sissano, Papua New Guinea tsunami of July 1998: offshore evidence on the source mechanism, Marine Geology, v. 175, pp. 1–23. doi:10.1016/S0025-3227(01)00131-1

Tappin, D.R., and Grilli, S.T., 2020, The continuing underestimated tsunami hazard from submarine landslides. In: Sassa K, Mikoš M, Sassa S, Bobrowsky PT, Takara K, Dang K (eds) Understanding and Reducing Landslide Disaster Risk: Volume 1 Sendai Landslide Partnerships and Kyoto Landslide Commitment. Part III Landslide-induced Tsunamis. Springer Nature. pp. 343–350

Tappin, D.R., 2021, Submarine Landslides and Their Tsunami Hazard. Annual Review of Earth and Planetary Sciences, v. 49, pp. 551–578. doi:10.1146/annurev-earth-063016-015810

Tinti, S., Manucci, A., Pagnoni, A., Armigliato., and Zaniboni, F., 2005, The 30 December 2002 landslide-induced tsunamis in Stromboli: sequence of the events reconstructed from the eyewitness accounts. Natural Hazards and Earth System Sciences, v. 5, pp. 763–775. doi:10.5194/nhess-5-763-2005

Whelan, M., 1994, The night the sea smashed Lord's Cove, Canadian Geographic, v. 114, pp. 70–73.

Shinji Sassa is Head of Soil Dynamics Group and Research Director of International Research Center for Coastal Disasters, Port and Airport Research Institute, National Institute of Maritime, Port and Aviation Technology, Japan. His expertise includes Scour and Erosion, Landslides and Tsunamis as Multi-Geohazards. He is the recipient of numerous distinguished awards, including the Prime Minister's Commendations for Disaster Prevention Merit, Outstanding Research Accomplishment Award, National Land Technology Development Award, and several Editor Awards for leading international journals. His Liquefaction Prediction and Assessment Paper was Top-Read Paper in ASCE Most Read Articles 2017-2021, and his Landslide-induced Tsunami paper is the most cited paper on Landslides and Tsunamis in Journal Landslides. He is currently Principal Coordinator of the International Union of Geological Sciences (IUGS) Task Group on Submarine Geohazards, Acting Executive Director of the International Consortium on Landslides (ICL), Chair of the International Consortium on Landslides (ICL) Network Committee, and Chair of the International Society for Soil Mechanics and Geotechnical Engineering (ISSMGE) Technical Committee on Scour and Erosion.

David Tappin is Principal Researcher at the British Geological Survey, where he leads Tsunami Hazard research, and Honorary Professor in the Earth Sciences Department at University College, London. He is a marine geologist specialising in submarine landslide and volcanic tsunamis and their onland sedimentary signatures. His research on the Papua New Guinea event of 1998 was seminal in proving the hazard from submarine landslide tsunamis. Since this time, he has researched all recent major tsunami events including those in the Indian Ocean (2004) and Japan (2011). Most recently he has been researching the Krakatau and Anak Krakatau tsunamis of 1883 and 2018. His research is internationally recognised and is extensively cited.

Hajime Naruse is Professor at Kyoto University (KU) and is a leading researcher in geohazard sediment transport. Naruse specialises in the use of AI in inversion of flow processes from geologic records, including ancient tsunami deposits. His expertise covers geological surveys of turbidites and tsunami deposits, numerical modelling and flume experiments of suspended sediment transport. Naruse has conducted field surveys of modern tsunami deposits, including the 2011 Tohoku-Oki and 2004 Indian Ocean events. Naruse is a director of JpGU.

Andreas Roulund is Senior Lead Specialist at Ørsted, a global leader in renewable energy solutions. As a practicing coastal engineer, Roulund has been involved in a diverse range of coastal engineering projects and their engineering design and project management across the globe. His paper on the numerical and experimental investigation of flow and scour around a circular pile published in Journal of Fluid Mechanics has been extensively cited worldwide. Roulund is a Corresponding Member representing Denmark of the International Society for Soil Mechanics and Geotechnical Engineering Technical Committee on Scour and Erosion.